NACA

RESEARCH MEMORANDUM

EFFECT OF PROPERTIES OF PRIMARY FLUID ON PERFORMANCE

OF CYLINDRICAL SHROUD EJECTORS

By Fred D. Kochendorfer

Lewis Flight Propulsion Laboratory
Cleveland, Ohio

NATIONAL ADVISORY COMMITTEE
FOR AERONAUTICS
WASHINGTON
March 11, 1954

NATIONAL ADVISORY COMMITTEE FOR AERONAUTICS

RESEARCH MEMORANDUM

EFFECT OF PROPERTIES OF PRIMARY FLUID ON PERFORMANCE

OF CYLINDRICAL SHROUD EJECTORS

By Fred D. Kochendorfer

SUMMARY

The effects of the properties of the primary fluid on ejector performance are examined both theoretically and experimentally. Experimental effects are determined by comparing the results obtained for a carbon dioxide primary with those obtained from previous tests with air. Comparisons are made for a series of cylindrical shroud ejectors having diameter ratios varying from 1.1 to 1.6, shroud lengths up to 1.0 primary diameter, and weight-flow ratios up to 0.13.

At primary pressure ratios for which the shroud is choked, density changes can be compensated by use of a weight-flow parameter equal to the weight-flow ratio multiplied by the square root of the temperature ratio and divided by the square root of the molecular weight ratio. The effect of specific heat ratio appears to be small, a change from 1.4 to 1.3 decreasing the weight-flow parameter by an amount which averaged about 0.005.

A theoretical analysis is also included to show that the effects of heat transfer between the primary and secondary streams can be large.

INTRODUCTION

Current interest in the air ejector both as a cooling air pump for afterburners and tail pipes and as a high-thrust nozzle for high-speed flight has led to the accumulation of a considerable quantity of performance data (see, for example, refs. 1 to 8). Since these investigations were chiefly exploratory in nature with a large number of configurations tested, small models and cold primary air were employed. Application of these data to full-scale turbojet installations requires a knowledge of the effects of scale and of primary gas temperature; and although the effect of scale is shown to be small for cold jets in reference 8, the effect of primary gas temperature is not yet clear.

For relatively short ejectors of the type used in aircraft, mixing effects may be small. Thus, it may be possible that quantities such as jet velocity, density, and viscosity which are associated with mixing and are dependent on temperature will have a negligible effect on ejector performance. The theory of reference 7 indicates that for pressure ratios sufficiently high for shroud choking and in the absence of mixing and heat transfer, temperature effect can be compensated by choosing as a weight-flow parameter a quantity equal to the secondary-to-primary weight-flow ratio multiplied by the square root of the secondary-to-primary temperature ratio. In addition, the experimental results of reference 9 substantiate the validity of this parameter at low pressure ratios and moderate temperatures. In the investigation of reference 8, on the other hand, attempts to correlate high-temperature, full-scale data with cold, small-scale data were unsuccessful. Factors which may have prevented the correlation were the differences in geometry between full scale and model, heat transfer between the primary and secondary streams, and the change in properties of the primary stream resulting from the temperature increase.

The purpose of the present investigation is to determine theoretically and experimentally the effect on ejector performance of changes in properties such as specific heat ratio and molecular weight. Dry air and carbon dioxide having specific heat ratios of 1.4 and 1.3 and molecular weights of 29 and 44, respectively, were used as the primary fluids.

Pumping characteristics are presented for cylindrical ejectors having secondary-to-primary diameter ratios ranging from 1.1 to 1.6 and shroud lengths up to 1 primary diameter. The range of weight-flow parameter was from 0 to 0.135.

APPARATUS AND PROCEDURE

The ejector apparatus schematically shown in figure 1 consisted of a primary chamber, four interchangeable primary nozzles, a plate containing the outer wall of the secondary nozzle, a secondary chamber, and a number of cylindrical interlocking shroud rings. (The definitions of symbols on fig. 1 and elsewhere are given in appendix A.) The arrangement was essentially that of reference 7 with the addition of a primary chamber.

All shroud rings had an inside diameter of 1.40 inches. Shroud length could be varied from 0 to 4.0 inches in 0.25-inch increments. The throat diameters of the primary nozzles were such that the available secondary-to-primary diameter ratios were 1.10, 1.20, 1.40, and 1.60.

Preliminary tests showed that the total pressures of the primary and secondary fluids at the nozzle exits were within 0.5 percent of those measured in the primary and secondary chambers for all conditions of operation. Chamber pressures were therefore used as a measure of total pressures.

The ejector assembly was mounted on a low-pressure receiver which was connected to the laboratory exhaust system. Any pressure between 2 inches of mercury and atmospheric could be obtained by throttling. Jet ambient pressure was measured by four static orifices in the receiver wall.

Atmospheric air was used for the secondary fluid. The air passed through a calibrated rotameter and a throttling valve and was then divided into two streams that entered the secondary chamber at diametrically opposite points.

Two different fluids were used for the primary: dry air and carbon dioxide. Air (dewpoint $-15^{\circ} \pm 5^{\circ}$ F) was obtained from the laboratory driers; carbon dioxide was supplied through the system shown schematically in figure 2. Liquid carbon dioxide was metered through an orifice into the steam heater; the carbon dioxide left this heater as a gas, was heated to $70^{\circ} \pm 10^{\circ}$ F in the auxiliary heater, passed through a flow-measuring orifice, and then divided into two streams that entered the primary chamber at opposite points.

For each configuration data were obtained by holding the secondary weight flow constant and varying the jet ambient pressure in steps from a low value to a value such that the primary nozzle was just choking. For each value of the ambient pressure, readings of the primary and secondary total pressures were taken.

RESULTS AND DISCUSSION

The experimental ejector performance curves are presented in figures 3, 4, 5, and 6 for shroud-to-nozzle diameter ratios of 1.10, 1.20, 1.40, and 1.60, respectively. For each curve ejector pressure ratio P_s/P_p is plotted as a function of primary pressure ratio p_0/P_p for a constant value of weight-flow parameter $\omega\sqrt{\tau/\mu}$, which is defined as the ratio of secondary-to-primary weight flow multiplied by the square root of the secondary-to-primary total temperature and divided by the square root of the secondary-to-primary molecular weight. With CO_2 as the primary fluid and air as the secondary, the value of μ is 0.653.

An inspection of the performance curves shows that for the lower values of primary pressure ratio, the ejector pressure ratio for each

curve is independent of the primary pressure and represents the minimum value obtainable for the particular value of the weight-flow parameter. As primary pressure ratio is increased a value called the break-off pressure ratio is reached for which the ejector pressure begins to increase. At break-off the abruptness of the change in ejector pressure ratio depends on the amount of secondary flow and decreases with increasing values of the weight-flow parameter. Above break-off, ejector pressure ratio increases almost linearly with primary pressure ratio.

These performance characteristics are, of course, similar to those which have been described in detail for the air ejector in reference 7. In the present report, for completeness, the description will be briefly repeated. At low primary pressure ratios the primary stream expands to a supersonic velocity on leaving the nozzle. For the case with no secondary flow the expansion continues until the jet completely fills the shroud and the resulting flow is sufficiently stable to withstand large pressure gradients near the shroud exit. The ejector pressure ratio is therefore constant over a large range of primary pressure ratios. Since those points on the performance curves which lie below a 45° line through the origin represent internal shroud pressures which are lower than ambient, it is obvious that with the larger diameter ratio, longer shrouds the primary jet can be greatly overexpanded.

With secondary flow, the primary expansion is cushioned and restricted by the secondary stream. Values of minimum ejector pressure ratio are therefore higher. In addition, since the lower energy secondary stream cannot support large pressure gradients, static pressures within the shroud cannot fall much below the ambient pressure and little overexpansion can occur. Only in the longer shrouds is mixing sufficient to permit secondary pressures lower than ambient.

The effect of diameter ratio and shroud length on minimum ejector pressure ratio is presented in figures 7 and 8; the former represents the case without secondary flow and the latter, the case with secondary flow. Also included in these figures are the results of a theoretical analysis similar to that of reference 7 but expanded to include the effects of changes in specific heat ratio and molecular weight (see appendix B).

The curves are identical in form to those obtained with air as the primary fluid. In figure 7 it can be seen that as shroud length is increased, the minimum ejector pressure ratio for each diameter ratio increases rapidly until a length which will be defined as the "critical shroud length" is reached. Further increases in length beyond critical have relatively little effect. An explanation of these phenomena is as follows: For short shrouds the primary stream expands outward to the shroud exit. Increasing shroud length thus permits less primary expansion and results in higher ejector pressure ratios; however, as the

3139

3139

shroud length increases beyond critical the flow in the upstream portion
of the shroud is stabilized and ejector pressure ratio becomes indepen-
dent of shroud length. The curves also show that the amount of expan-
sion which can be accommodated governs the effect of diameter ratio in
a like manner. The smaller diameter shrouds allowing less expansion
produce higher values of minimum ejector pressure ratio.

Similar trends with secondary flow are apparent in figure 8. The
chief effect of secondary flow, other than that of increasing minimum
ejector pressure ratio levels, is an appreciable increase in critical
shroud length. With a diameter ratio of 1.2, for example, critical
shroud lengths are 0.27 and about 0.7 for operation without and with
secondary flow, respectively.

Inspection of the experimental and theoretical curves of figures 7
and 8 shows that the theory properly evaluates the effects of diameter
and weight-flow ratios for the case of stabilized shroud flow. In addi-
tion, for the case without secondary flow, the effect of shroud length
appears to check that predicted by the theory.

Effect of Fluid Properties on Ejector Performance

It has been shown that at pressure ratios sufficient for shroud
choking, the flow within the shroud becomes stabilized (for the diameter
ratios investigated) within a distance of about 1.0 primary diameter
downstream of the shroud exit, and it is therefore possible that mixing
and heat transfer effects may play an insignificant role in determining
the values of minimum ejector pressure ratio.

The results of a theoretical analysis based on this premise (see
appendix B) are presented in figure 9. It can be seen that the effect
of changes in the properties of the primary fluid cannot be completely
correlated by use of the weight-flow parameter $\omega \sqrt{\tau/\mu}$, since, although
the effect of density (ie, temperature or molecular weight) is accounted
for, that of specific heat ratio γ is not. The magnitude of the γ
effect evidently depends on both diameter and weight-flow parameter.
In general, decreasing γ from 1.4 to 1.3 shifts the curves toward the
lower weight-flow parameters; for the range of variables included in
figure 9 the shift amounts to about 0.01. For the smaller diameter ratio,
however, the slope is also decreased with the result that for $D_s/D_p = 1.1$
and for $\omega \sqrt{\tau/\mu} > 0.07$, weight-flow ratio is actually increased by a de-
crease in γ.

A set of performance curves similar to those of figure 9 but ob-
tained experimentally is presented in figure 10. The data for $\gamma_p = 1.3$
were obtained from the curves of figures 7 and 8; those for $\gamma_p = 1.4$

NACA RM E53L24a

were obtained both from the tests of a larger scale (primary diameter = 4
in.) investigation reported in reference 5 and from the apparatus of the
present investigation using dry air as the primary fluid. It can be seen
that the experimental trends are similar to the theoretical. Quanti-
tatively, however, the effect of γ is not so large, the shift in weight-
flow ratio averaging only 0.005. Therefore, at a weight-flow ratio of
about 0.04, the γ effect amounts to a 12 percent weight flow change at
constant minimum ejector pressure ratio. At constant weight flow, how-
ever, the effect on ejector pressure ratio is small, varying from about
3 to 5 percent.

At the higher pressure ratios for which the shroud is not choked,
there is no reason to believe that mixing and heat-transfer effects
should be insignificant. Thus, the weight-flow parameter cannot be ex-
pected a priori to correlate values of ejector pressure ratio for fluids
having different densities. Nevertheless, the experimental results of
reference 8 indicate that density effects (in this case resulting from
molecular weight change) can be found by comparing the results for CO_2
with those for air. This comparison for both $\omega \sqrt{T}/\mu$ and $\omega \sqrt{T}$ is
presented in figure 11 at a primary pressure ratio of 0.50. For the two
smaller diameter ratios, a better correlation obviously is obtained by
using $\omega \sqrt{T}/\mu$. Except for the case with zero secondary flow, the largest
weight-flow discrepancy is about 10 percent. For $D_s/D_p = 1.4$, since the
curves for different flows are closely spaced, data scatter makes evalua-
tion of results difficult.

Effect of Scale and Heat Transfer

In the investigations of reference 8 weight-flow ratios for a small
scale model having an unheated primary jet were found to exceed those of
a similar full-scale, heated jet ejector by as much as 200 percent.
Since the present investigation shows that such errors cannot result from
density or γ effects alone, the cause must have been differences in
geometry between full scale and model or in heat transfer.

The extreme sensitivity of weight flow to ejector pressure ratio at
a high value of primary pressure ratio p_0/P_p has been noted in figure
11. At a diameter ratio of 1.2 and a shroud length of 0.5, for example,
changing the ejector pressure ratio by 4 percent (from 0.50 to 0.52)
doubles the secondary flow. Therefore, the geometry of the secondary
passage just upstream of the shroud entrance and the location of the
measuring station for P_s are particularly important.

The effect of heat transfer on ejector performance cannot be deter-
mined because the amount of heat which can be transferred between the
primary and secondary streams within the relatively short aircraft ejector

shrouds is not known at present. However, the effect of a given amount of heat transfer can be found theoretically. Using the theory of appendix B, calculations have been made for the following case: secondary-to-primary temperature ratio τ, 1/4; ratio of secondary temperature at shroud exit to that at shroud entrance τ_s, 2; $\gamma_p = \gamma_s = 1.4$. The results are compared with those for no heat transfer ($\tau_s = 1$) in figure 12. The effect of heat transfer is similar to that of γ change in that the curves are shifted to lower values of weight flow. For the assumed conditions the effect is to approximately halve the secondary flow. Although this is in the proper direction to explain the results of reference 8, no quantative answers can be given because, as has been mentioned, the proper value for τ_s is unknown. With respect to figure 12, it should be noted that for a given ejector τ_s will, in general, vary with secondary flow. If the amount of heat transferred remains constant, τ_s will vary inversely with secondary flow; therefore the effect on ejector pressure ratio should be smaller for the higher secondary flows. This trend was evident in the data.

From the foregoing discussion it is apparent that a change in the properties of the primary fluid should have little effect on ejector performance if $\omega\sqrt{\tau}/\mu$ is used as the weight-flow parameter. If temperature changes accompany the property changes, however, the effect of heat transfer can result in large discrepancies. Furthermore, at pressure ratios for which the shroud is not choked, slight differences in geometry can also greatly affect secondary flow.

SUMMARY OF RESULTS

The following results were obtained from a small-scale investigation to determine the effects of properties of the primary fluid on ejector performance:

1. At primary pressure ratios for which the shroud was choked, decreasing specific heat ratio γ from 1.4 to 1.3 decreased the weight-flow parameter $\omega\sqrt{\tau}/\mu$ by 0.005 or less for diameter ratios from 1.1 to 1.6. At constant weight flow the effect on ejector pressure ratio was small.

2. When the shroud was not choked, the effect of γ appeared to be small and the weight-flow parameter seemed to correlate performance data. However, because of the extreme sensitivity of weight-flow ratio to ejector pressure ratio, data scatter may have been sufficient to mask the effects of changes in fluid properties.

3. The effects of heat transfer between the primary and secondary
fluids can be large. Consequently, if the shroud is long enough to
permit appreciable heat transfer, data obtained with a cold primary jet
cannot be expected to accurately predict those for a heated jet.

Lewis Flight Propulsion Laboratory
    National Advisory Committee for Aeronautics
        Cleveland, Ohio, December 16, 1953

3139

3139

63-2

APPENDIX A

SYMBOLS

A   area

A/A^* $\dfrac{1}{M}\sqrt{\left[\dfrac{2}{\gamma+1}\left(1+\dfrac{\gamma-1}{2}M^2\right)\right]^{\frac{\gamma+1}{\gamma-1}}}$

a   area ratio, A_s/A_p

b   area ratio, A_l/A_p

D   diameter

F/F^* $\dfrac{1+\gamma M^2}{M\sqrt{2(\gamma+1)\left(1+\dfrac{\gamma-1}{2}M^2\right)}}$

g   acceleration due to gravity

K   loss constant

L   shroud length

$(L/D_p)_c$ critical shroud length

M   Mach number

m   molecular weight

P   total pressure

p   static pressure

$(P_s/P_p)_m$ minimum ejector pressure ratio

R   universal gas constant

T   total temperature

V   velocity

w   weight flow

γ specific heat ratio

μ molecular weight ratio, m_s/m_p

ρ density

τ temperature ratio, T_s/T_p

τ_s temperature ratio, T_2/T_s

ω weight-flow ratio, w_s/w_p

Subscripts:

p   primary stream at nozzle exit

s   secondary stream at nozzle exit

0   jet ambient

1   primary stream at shroud station for which primary and secondary static pressures are equal

2   secondary stream at shroud station for which primary and secondary static pressures are equal

APPENDIX B

EJECTOR THEORY

No Secondary Flow

<u>Shroud length ratios greater than critical</u>. - The one-dimensional equations for the conservation of mass and momentum will be written for the section of the shroud between stations I and II.
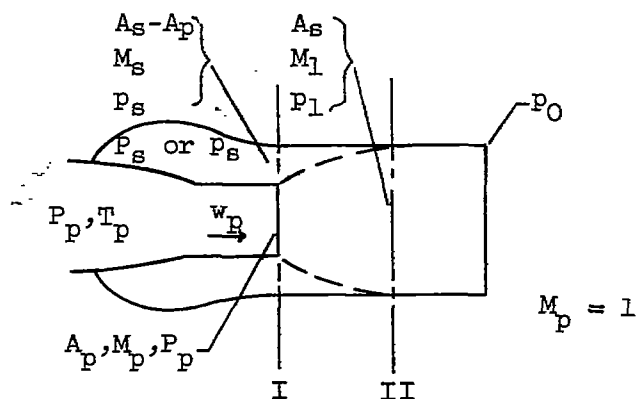
Let $a = \dfrac{A_s}{A_p} \equiv \left(\dfrac{D_s}{D_p}\right)^2$. The equation for the conservation of mass is then

$$w_p = w_1$$

or

$$P_p \sqrt{\frac{\gamma_p + 1}{2}} = a p_1 M_1 \sqrt{1 + \frac{\gamma_1 - 1}{2} M_1^2} \tag{1}$$

The equation for conservation of momentum is

$$p_p + \rho_p V_p^2 + (a - 1)p_s = a p_1 + a \rho_1 V_1^2$$

or

$$p_p (1 + \gamma_p) + (a - 1)p_s = a p_1 (1 + \gamma_1 M_1^2) \tag{2}$$

Assumptions will be made as follows:

(1) Adiabatic flow, $T_p = T_1$

(2) $\gamma_p = \gamma_1 = \gamma$

(3) The shear on the expanding primary stream results in a pressure change which is given by

$$p_1 - p_s = K \frac{\rho_1 V_1^2}{2}$$

or

$$p_1 - p_s = K \frac{\gamma}{2} p_1 M_1^2$$

With these assumptions equations (1) and (2) can be rearranged in the following form:

$$\frac{a - 1}{2a} = \frac{\left(\frac{F}{F^*}\right)_1 - 1}{\left(\frac{K}{2} + 1\right)\left(\frac{\gamma + 1}{2}\right)^{\frac{1}{\gamma - 1}} \left(\frac{A}{A^*}\right)_1 \frac{p_1}{p_1} - K\left(\frac{F}{F^*}\right)_1} \qquad (3)$$

$$\frac{P_s}{P_p} \equiv \frac{p_s}{p_p} = \sqrt{\left(\frac{2}{\gamma + 1}\right)^{\frac{\gamma+1}{\gamma-1}} \frac{1 - K \frac{\gamma}{2} M_1^2}{aM_1 \sqrt{1 + \frac{\gamma - 1}{2} M_1^2}}} \qquad (4)$$

If the value of K is either known or assumed, for each M_1 values can be obtained for both a and P_s/P_p. Therefore P_s/P_p is determined as a function of a (or D_s/D_p) and K.

Shroud length ratios less than critical. - Assume that the primary fluid undergoes a Prandtl-Meyer expansion such that it just strikes the shroud exit. Assume also that for the diameter ratios under consideration two-dimensional flow is sufficiently accurate.

Then $(P_s/P_p)_m$ is the pressure ratio corresponding to an expansion through an angle v (see, for example, ref. 10) where

$$v = \tan^{-1} \frac{D_s/D_p - 1}{2L/D_p}$$

The ratio $(P_s/P_p)_m$ is thus a known function of D_s/D_p and L/D_p.

Secondary Flow

The one-dimensional equations for the conservation of mass and momentum will again be written for the section of the shroud between stations I and II.
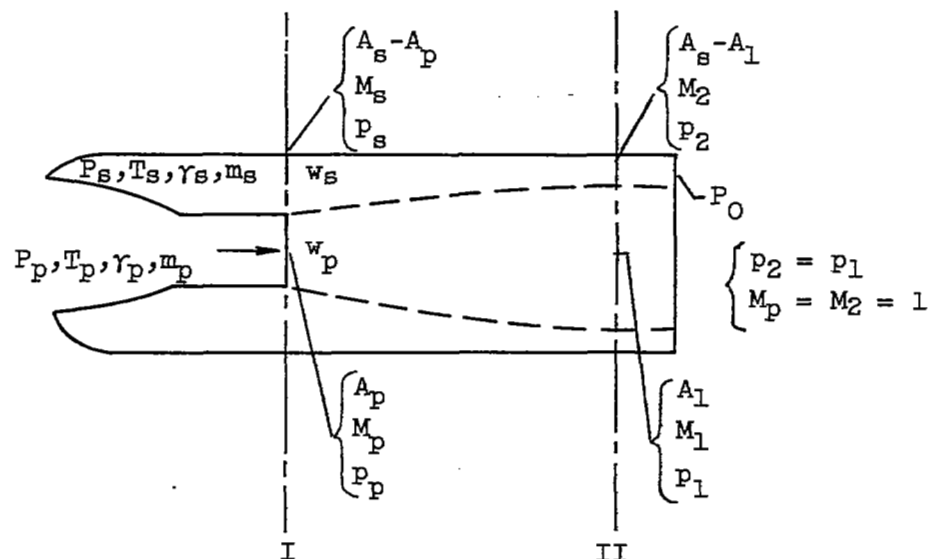
Let $a = A_s/A_p$ and $b = A_1/A_p$; conservation of mass for the primary stream is then

$$\sqrt{\frac{R}{g}}\, w_p = A_p \sqrt{\gamma_p m_p}\, \frac{p_p}{\sqrt{T_p}} \sqrt{\frac{\gamma_p + 1}{2}} = bA_p \sqrt{\gamma_1 m_p}\, \frac{p_1}{\sqrt{T_1}}\, M_1 \sqrt{1 + \frac{\gamma_1 - 1}{2} M_1^2}$$

and for the secondary stream,

$$\sqrt{\frac{R}{g}}\, w_s = (a - 1)A_p \sqrt{\gamma_s m_s}\, \frac{p_s}{\sqrt{T_s}} \sqrt{1 + \frac{\gamma_s - 1}{2} M_s^2} = (a - b)A_p \sqrt{\gamma_s m_s}\, \frac{p_1}{\sqrt{T_2}} \sqrt{\frac{\gamma_2 + 1}{2}}$$

Conservation of momentum for the combined flow neglecting shroud wall friction forces is given by

$$p_p(1 + \gamma_p) + (a - 1)p_s(1 + \gamma_s M_s^2) = bp_1(1 + \gamma_1 M_1^2) + (a - b)p_1(1 + \gamma_2)$$

This equation can be rewritten as follows:

$$\omega\sqrt{\frac{\tau}{\mu}} = \frac{\sqrt{\frac{\gamma_1 + 1}{\gamma_1}}\left(\frac{F}{F^*}\right)_1 - \sqrt{\frac{\gamma_p + 1}{\gamma_p}}}{\sqrt{\frac{\gamma_s + 1}{\gamma_s}}\left(\frac{F}{F^*}\right)_s - \sqrt{\tau_s}\sqrt{\frac{\gamma_2 + 1}{\gamma_2}}} \tag{8}$$

and equations (5) and (6), as

$$\omega\sqrt{\frac{\tau}{\mu}} = (a - 1)\sqrt{\frac{\gamma_s}{\gamma_p}}\sqrt{\left(\frac{2}{\gamma_s + 1}\right)^{\frac{\gamma_s+1}{\gamma_s-1}}}\sqrt{\left(\frac{\gamma_p + 1}{2}\right)^{\frac{\gamma_p+1}{\gamma_p-1}}}\frac{P_s}{P_p}\frac{1}{\left(\frac{A}{A^*}\right)_s}$$

$$= (a - b)\sqrt{\frac{1}{\tau_s}}\sqrt{\frac{\gamma_2(\gamma_2 + 1)}{\gamma_p(\gamma_p + 1)}}\left(\frac{\gamma_p + 1}{2}\right)^{\frac{\gamma_p}{\gamma_p-1}}\frac{p_1}{P_p} \tag{9}$$

For known or assumed values of γ and τ_s, equation (8) determines $\omega\sqrt{\tau/\mu}$ as a function of M_1 and M_s. Equation (9) similarly determines the quantities $(a - 1)\dfrac{P_s}{P_p}$ and $(a - b)\dfrac{p_1}{P_p}$. If b and $\dfrac{p_1}{P_p}$ can be found as functions of M_1 and M_s, a relation will be established between $\omega\sqrt{\tau/\mu}$, $\dfrac{P_s}{P_p}$, and a.

In the theory of reference 7, the primary expansion was assumed to be isentropic; thus b and p_1/p_p were determined as functions of M_1. In the present treatment, it will be assumed that because of shear between the primary and secondary streams, p_1 differs from its isentropic value by an amount which is given by

$$(p_1)_{isen} - p_1 = p_1\frac{\gamma}{2}K(M_1^2 - M_2^2)$$

3139

or

$$\frac{p_1}{P_p} = \frac{p_1/P_1}{1 + \frac{\gamma}{2} K(M_1^2 - 1)} \tag{10}$$

and the value for b is then

$$b = \left(\frac{A}{A^*}\right)_1 \times 1 + \frac{\gamma}{2} k(M_1^2 - 1) \times \frac{T_1}{T_p} \tag{11}$$

where the temperature ratio T_1/T_p can be found from the energy equation

$$\frac{R}{m_p} \frac{\gamma_p}{\gamma_p - 1} w_p(T_p - T_1) = \frac{R}{m_s} \frac{\gamma_s}{\gamma_s - 1} w_s(T_2 - T_s)$$

or

$$\frac{T_1}{T_p} = 1 - \omega \sqrt{\frac{T}{\mu}} \sqrt{\frac{T}{\mu}} \frac{\gamma_s}{\gamma_s - 1} \frac{\gamma_p - 1}{\gamma_p} (\tau_s - 1) \tag{12}$$

Therefore, equation (9) becomes

$$a \equiv \left(\frac{D_s}{D_p}\right)^2 = \left[1 + \frac{\gamma}{2} K(M_1^2 - 1)\right] \left\{ \left(\frac{A}{A_1^*}\right) \left[1 - \omega\sqrt{\frac{T}{\mu}} \sqrt{\frac{T}{\mu}} \frac{\gamma_s}{\gamma_s - 1} \frac{\gamma_p - 1}{\gamma_p} (\tau_s - 1)\right] + \right.$$

$$\left. \omega\sqrt{\frac{T}{\mu}} \sqrt{T_s} \sqrt{\frac{\gamma_p(\gamma_p + 1)}{\gamma_2(\gamma_2 + 1)}} \left(\frac{2}{\gamma_p + 1}\right)^{\frac{\gamma_p}{\gamma_p - 1}} \frac{p_1}{P_1} \right\} \tag{13}$$

$$\frac{P_s}{P_p} = \omega \sqrt{\frac{T}{\mu}} \sqrt{\frac{\gamma_p}{\gamma_s}} \sqrt{\left(\frac{2}{\gamma_p + 1}\right)^{\frac{\gamma_p+1}{\gamma_p-1}}} \sqrt{\left(\frac{\gamma_s + 1}{2}\right)^{\frac{\gamma_s+1}{\gamma_s-1}}} \frac{\left(\frac{A}{A^*}\right)_s}{a - 1} \tag{14}$$

With equations (8), (13), and (14), values for $\omega\sqrt{\frac{T}{\mu}}$, D_s/D_p, and P_s/P_p are determined for any pair of values for M_s and M_1.

Calculations were made for a series of values for the loss parameter K. In a comparison with the experimental data it was found that a value of 0.07 seemed to provide the best fit. Therefore, this value was used for figures 7 to 9. In figure 12, no losses were assumed, that is, $K = 0$.

REFERENCES

1. Huddleston, S. C., Wilsted, H. D., and Ellis, C. W.: Performance of Several Air Ejectors with Conical Mixing Sections and Small Secondary Flow Rates. NACA RM E8D23, 1948.

2. Ellis, C. W., Hollister, D. P., and Sargent, A. F., Jr.: Preliminary Investigation of Cooling-Air Ejector Performance at Pressure Ratios from 1 to 10. NACA RM E51H21, 1951.

3. Greathouse, W. K., and Hollister, D. P.: Preliminary Air-Flow and Thrust Calibrations of Several Conical Cooling-Air Ejectors with a Primary to Secondary Temperature Ratio of 1.0. I - Diameter Ratios of 1.21 and 1.10. NACA RM E52E21, 1952.

4. Greathouse, W. K., and Hollister, D. P.: Preliminary Air-Flow and Thrust Calibrations of Several Conical Cooling-Air Ejectors with a Primary to Secondary Temperature Ratio of 1.0. II - Diameter Ratios of 1.06 and 1.40. NACA RM E52F26, 1952.

5. Greathouse, W. K., and Hollister, D. P.: Air-Flow and Thrust Characteristics of Several Cylindrical Cooling-Air Ejectors with a Primary to Secondary Temperature Ratio of 1.0. NACA RM E52L24, 1953.

6. Huntley, S. C., and Yanowitz, Herbert: Pumping and Thrust Characteristics of Several Divergent Cooling-Air Ejectors and Comparison of Performance with Conical and Cylindrical Ejectors. NACA RM E53J13, 1953.

7. Kochendorfer, Fred D., and Rousso, Morris D.: Performance Characteristics of Aircraft Cooling Ejectors Having Short Cylindrical Shrouds. NACA RM E51E01, 1951.

8. Wallner, Lewis E., and Jansen, Emmert T.: Full-Scale Investigation of Cooling Shroud and Ejector Nozzle for a Turbojet Engine-Afterburner Installation. NACA RM E51J04, 1951.

9. Wilsted, H. D., Huddleston, S. C., and Ellis, C. W.: Effect of Temperature on Performance of Several Ejector Configurations. NACA RM E9E16, 1949.

10. The Staff of the Ames 1- by 3-Foot Supersonic Wind-Tunnel Section: Notes and Tables for Use in the Analysis of Supersonic Flow. NACA TN 1428, 1947.
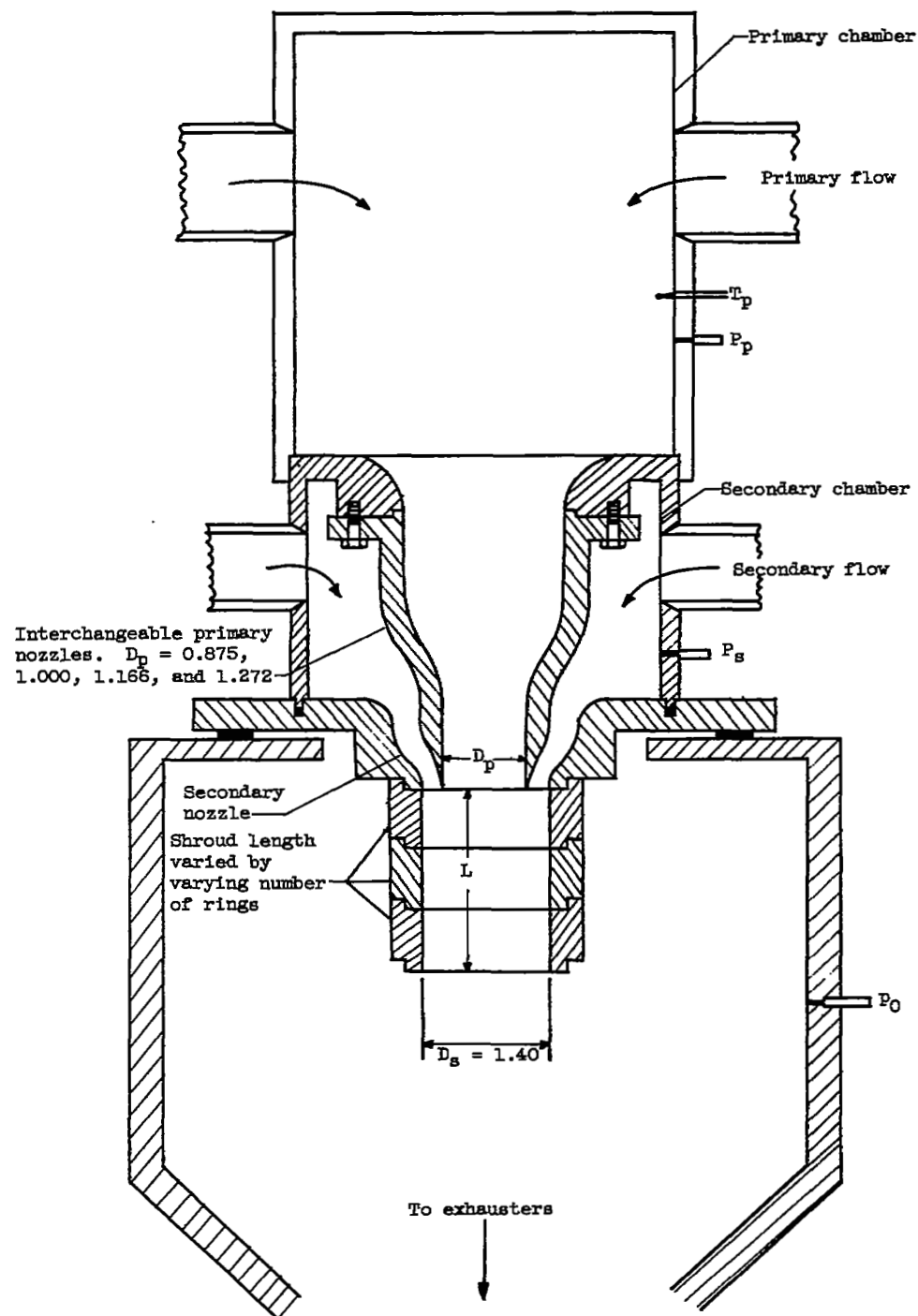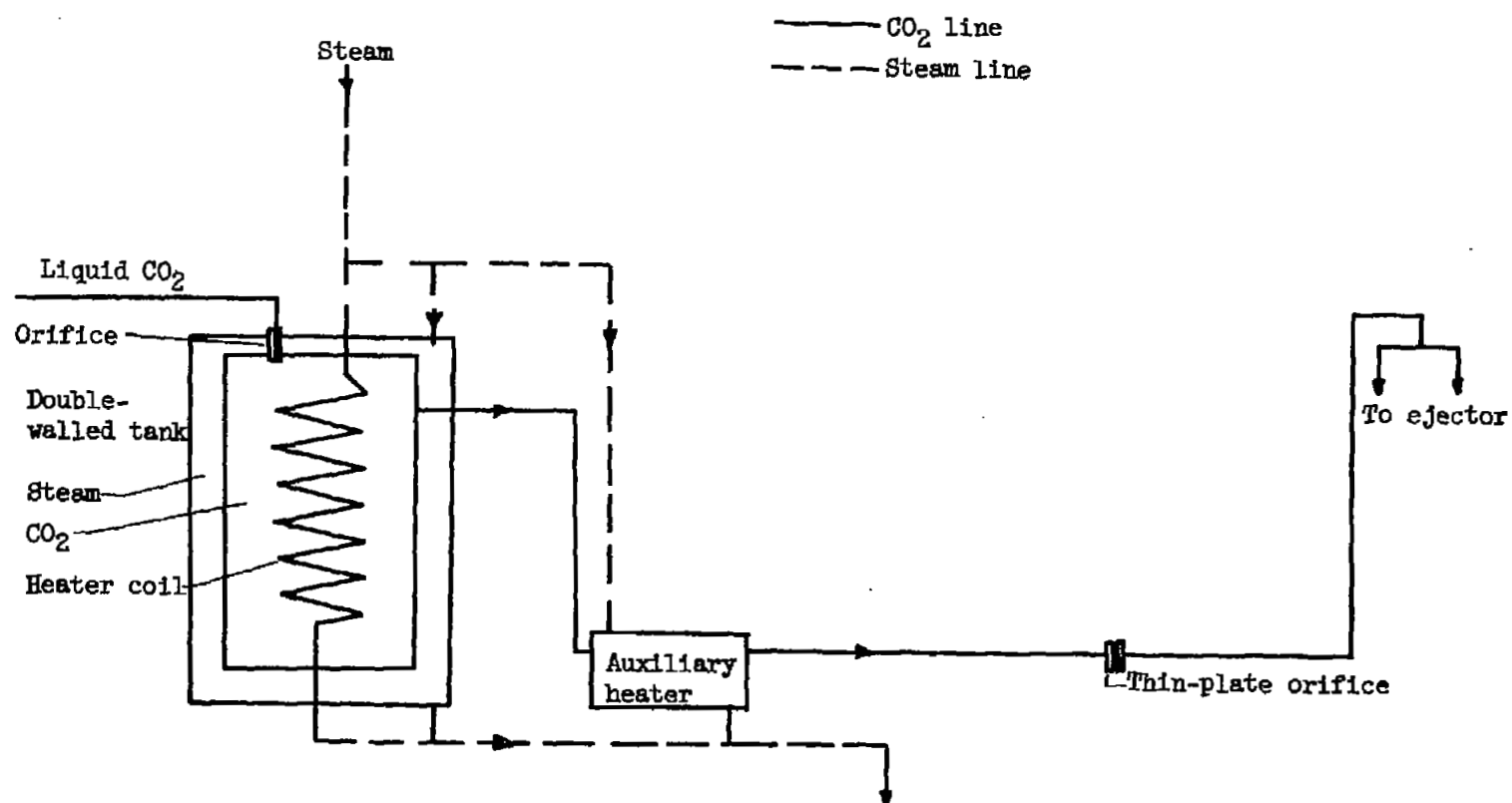
3139

CQ-3

Primary chamber

Primary flow

T_p

P_p

Secondary chamber

Secondary flow

Interchangeable primary nozzles. D_p = 0.875, 1.000, 1.166, and 1.272

P_s

D_p

Secondary nozzle

Shroud length varied by varying number of rings

L

D_s = 1.40

P_0

To exhausters

Figure 1. - Ejector apparatus.

CO$_2$ line

Steam line

Steam

Liquid CO$_2$

Orifice

Double-walled tank

Steam

CO$_2$

Heater coil

Auxiliary heater

To ejector

Thin-plate orifice

Figure 2. - Schematic flow diagram of carbon dioxide heating system.

(a) Shroud length ratio L/D_p, 0.39.

(b) Shroud length ratio L/D_p, 0.79.
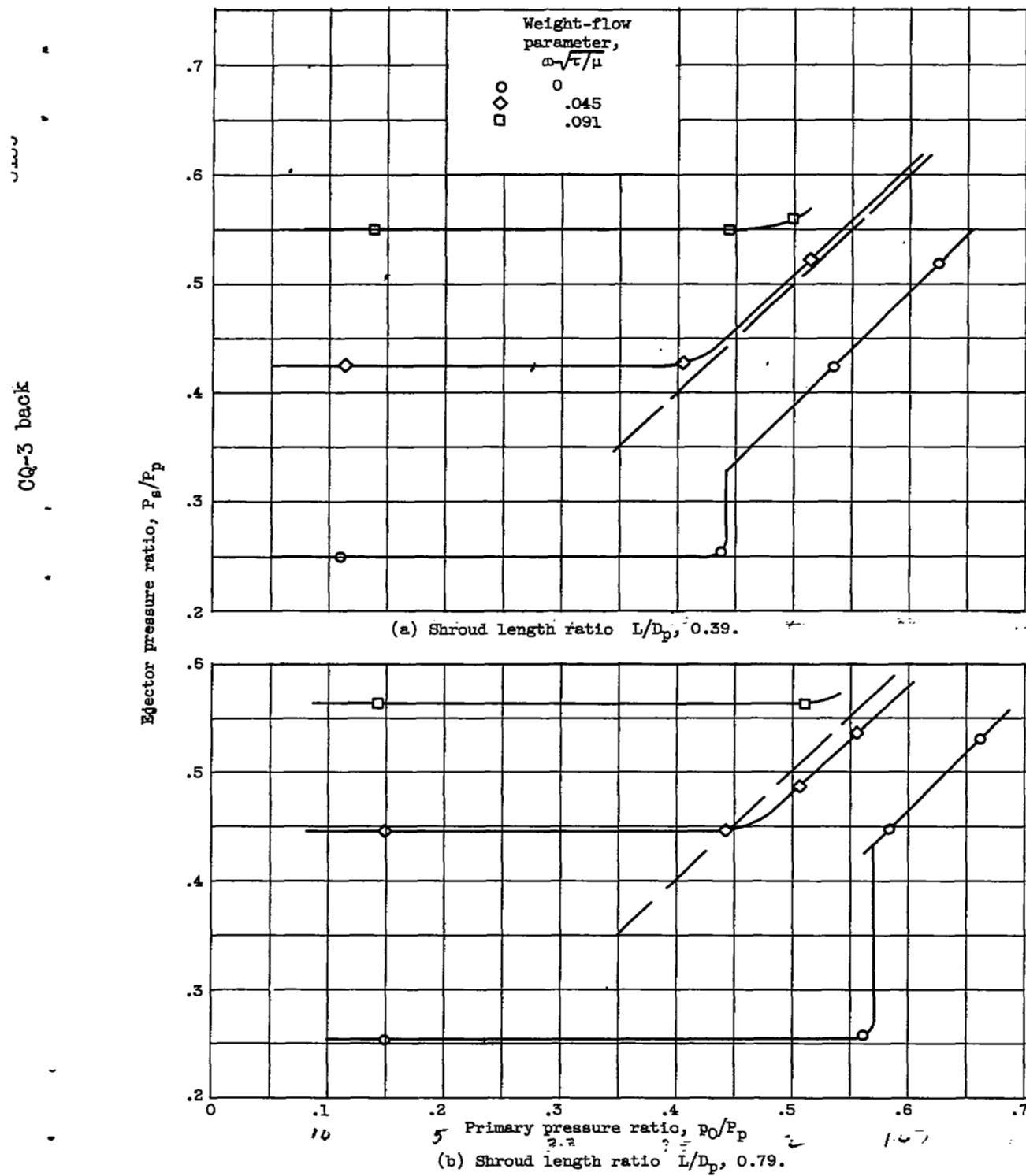
Figure 3. - Performance of carbon dioxide-air ejector with diameter ratio of 1.10.

(a) Shroud length ratio L/D_p, 0.43

(b) Shroud length ratio L/D_p, 0.64.
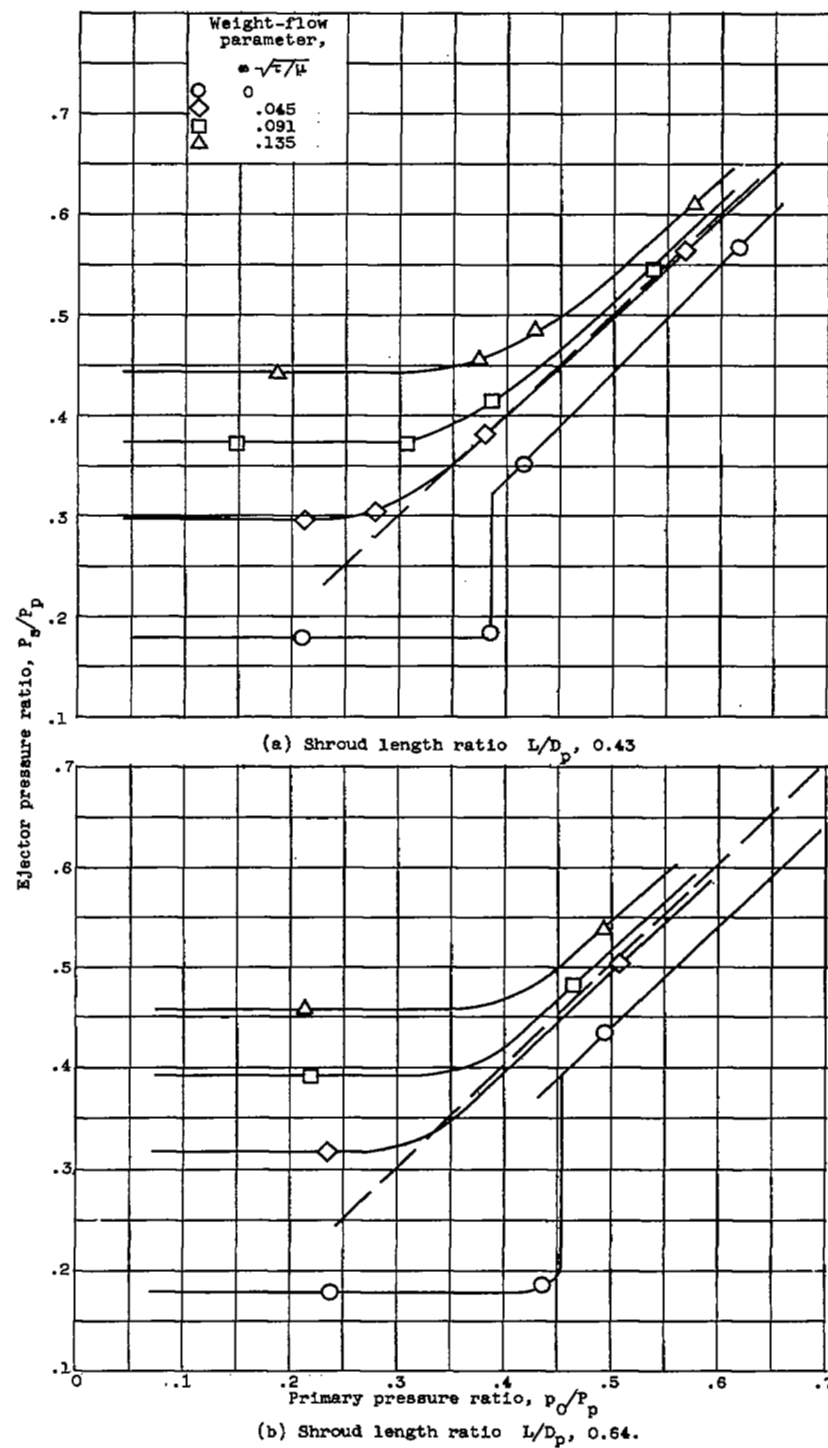
Figure 4. - Performance of carbon dioxide-air ejector with diameter ratio of 1.20.
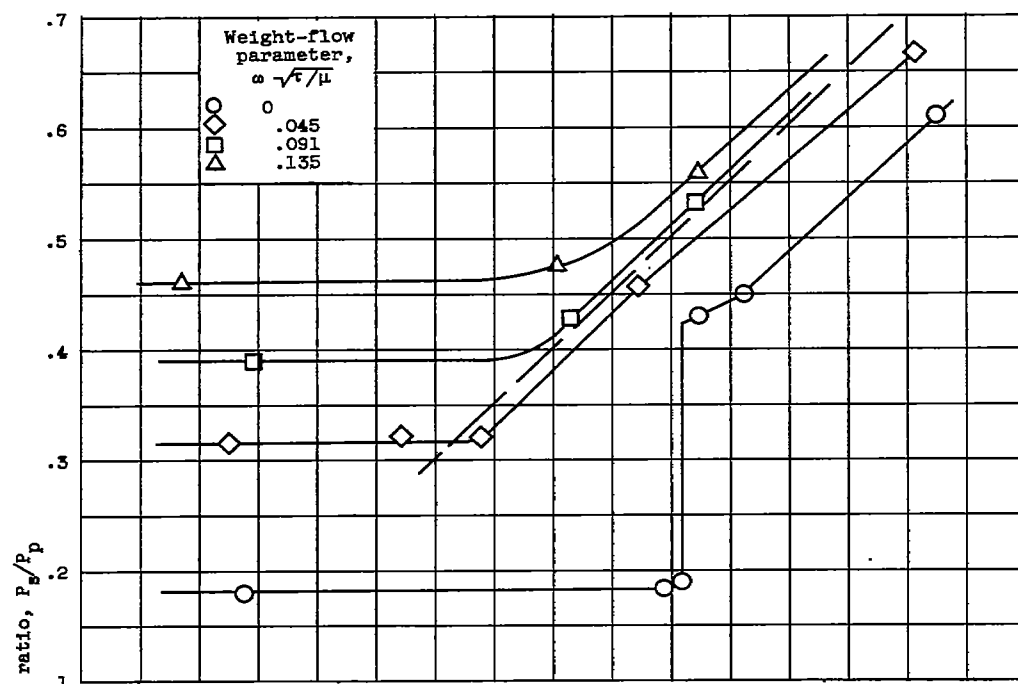
(c) Shroud length ratio L/D_p, 0.86.
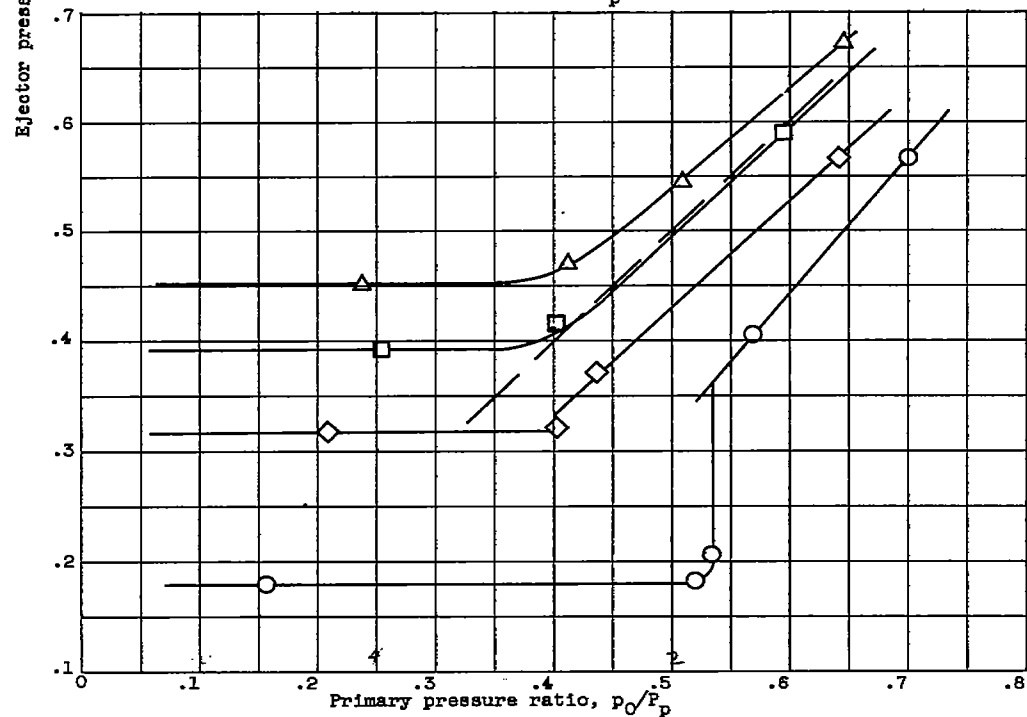
(d) Shroud length ratio L/D_p, 1.29.

Figure 4. - Concluded. Performance of carbon dioxide-air ejector with diameter ratio of 1.20.

(a) Shroud length ratio, L/D_p, 0.25.

(b) Shroud length ratio L/D_p, 0.50.
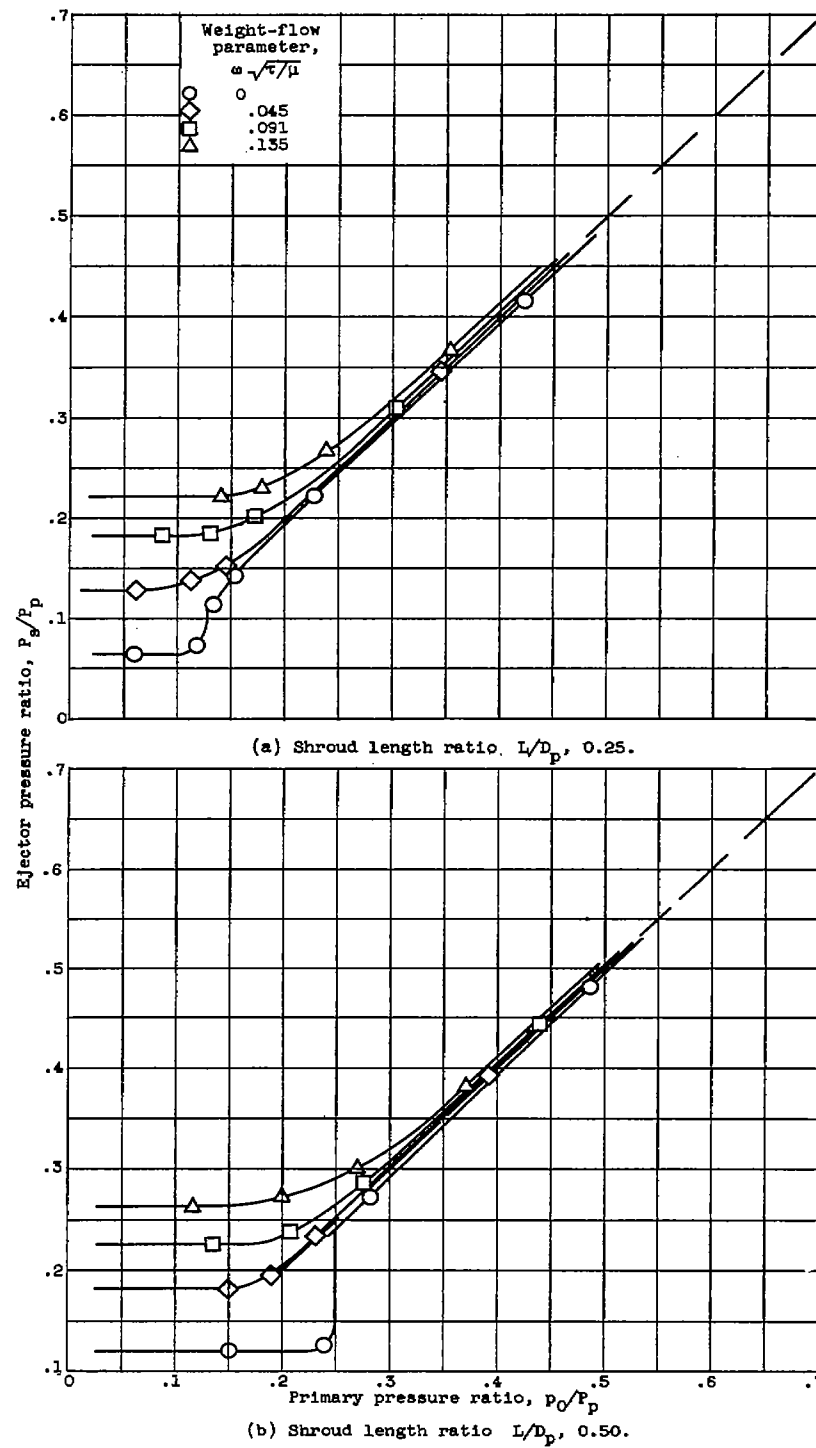
Figure 5. - Performance of carbon dioxide-air ejector with diameter ratio of 1.40.

3139·

Weight-flow parameter, $\omega \sqrt{\tau}/\mu$

○	0
◇	.045
□	.091
△	.135

(c) Shroud length ratio L/D_p, 0.75.

(d) Shroud length ratio L/D_p, 1.00.

Primary pressure ratio, p_0/P_p

Ejector pressure ratio, P_B/P_p
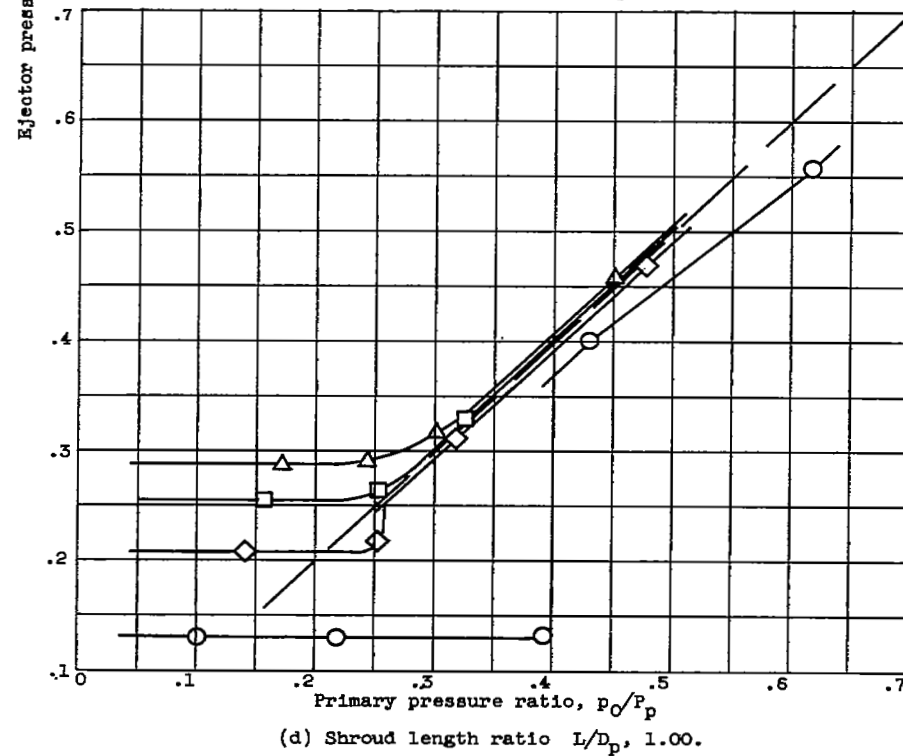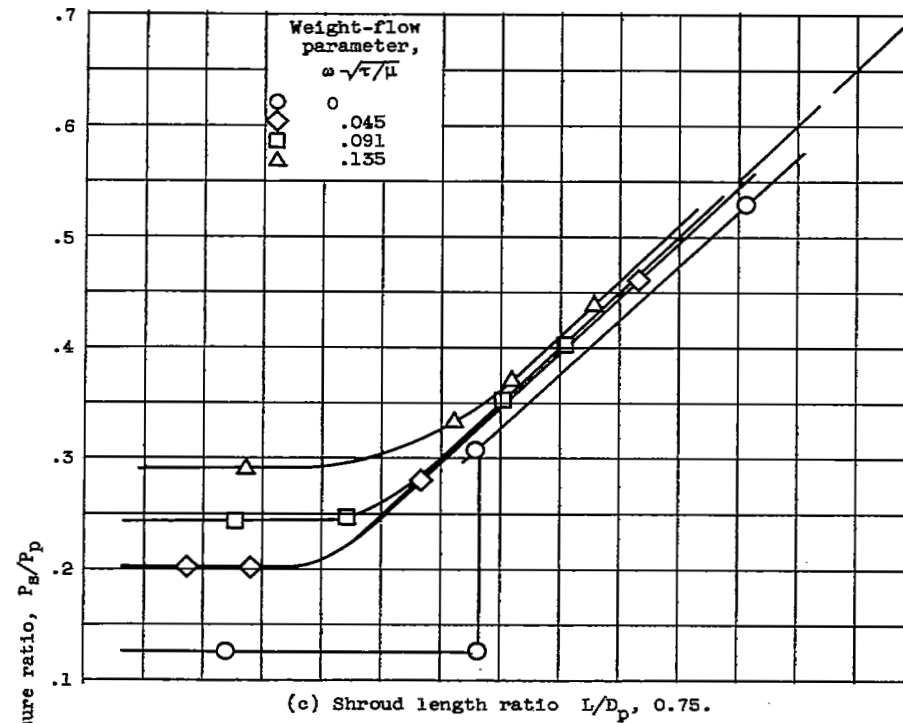
Figure 5. – Concluded. Performance of carbon dioxide-air ejector with diameter ratio of 1.40.
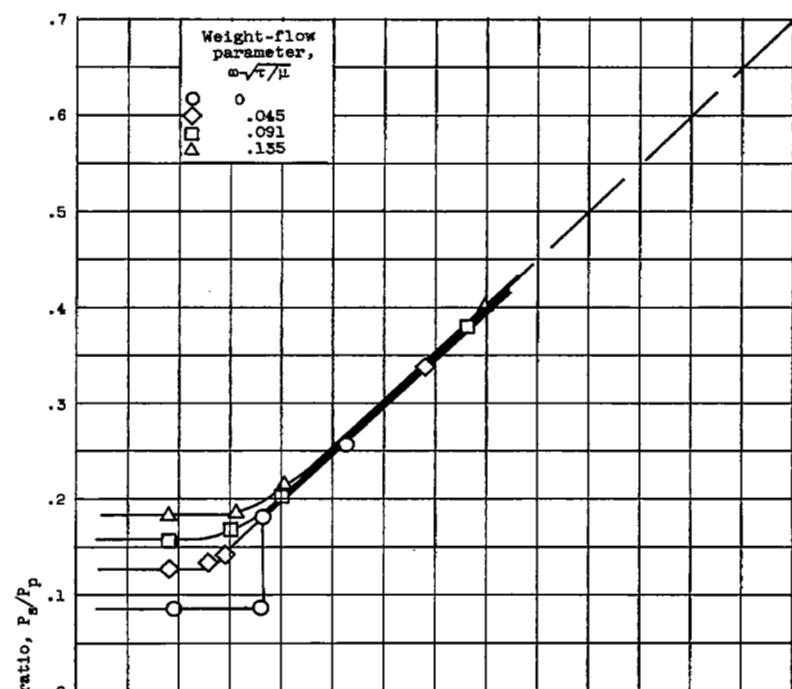
(a) Shroud length ratio L/D_p, 0.57.
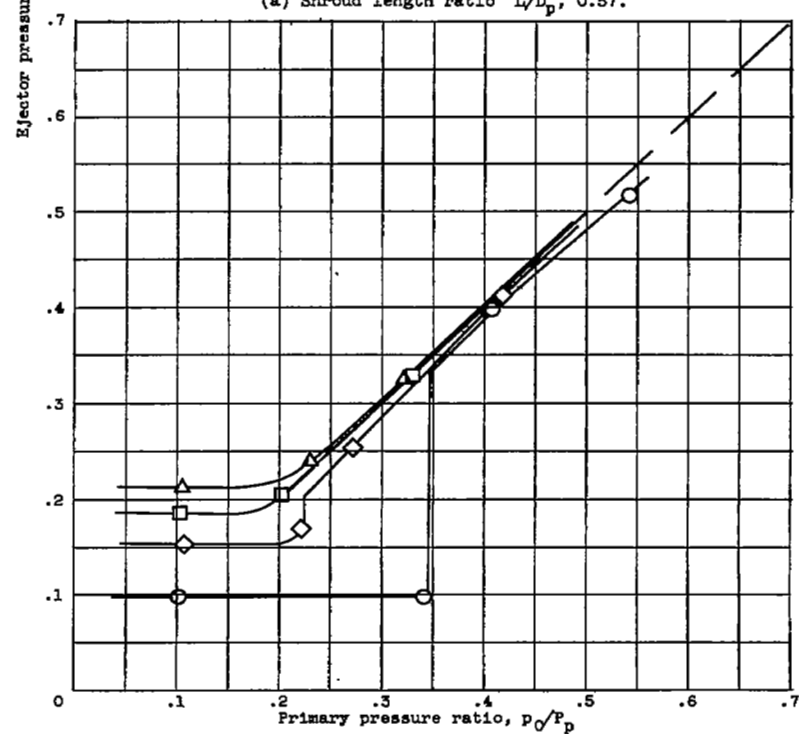
(b) Shroud length ratio L/D_p, 1.14.

Figure 6. - Performance of carbon dioxide-air ejector with diameter ratio of 1.60.
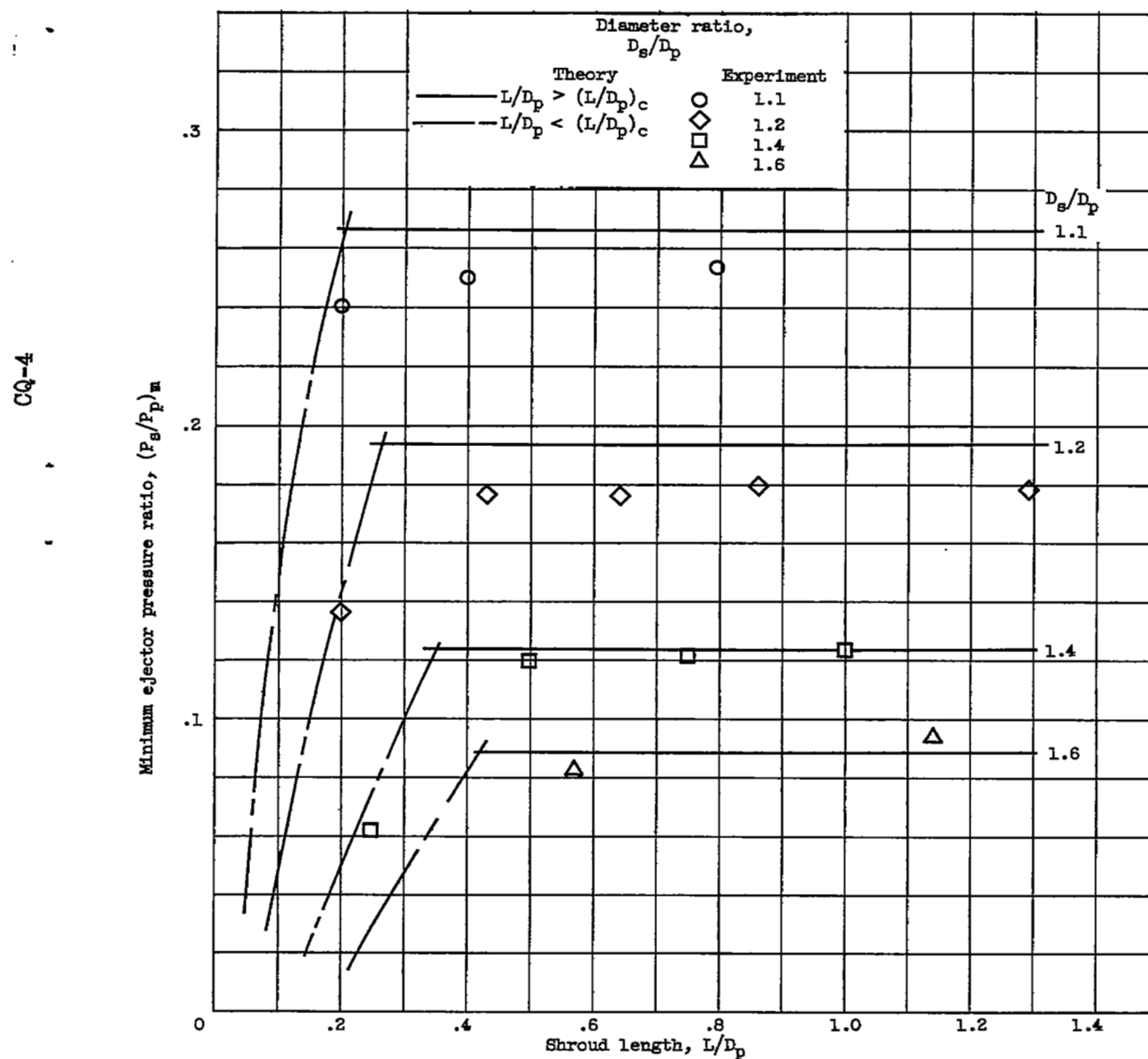
Figure 7. - Effect of diameter ratio and shroud length on minimum ejector pressure ratio with no secondary flow. Primary specific heat ratio, 1.3; secondary specific heat ratio, 1.4.
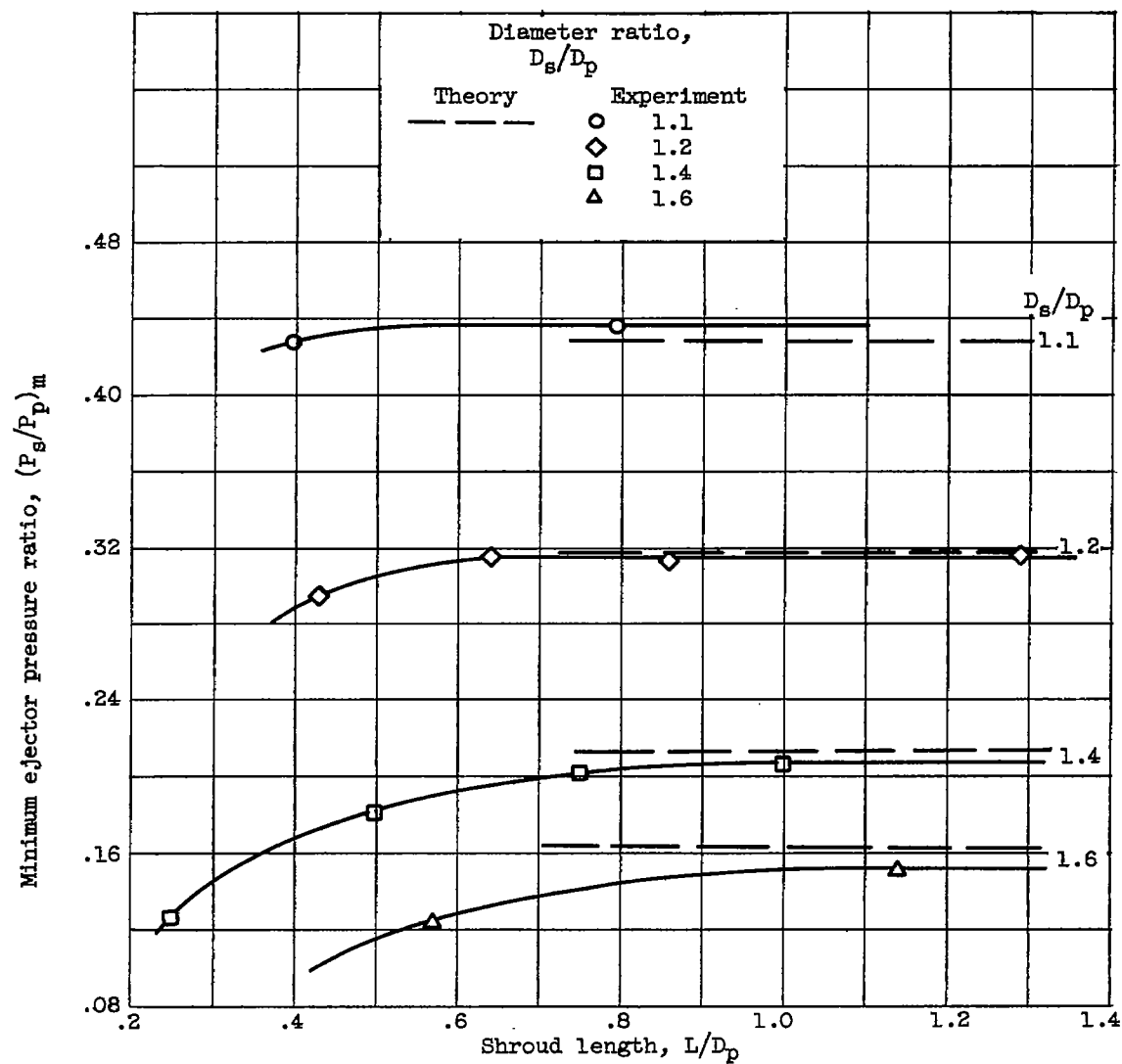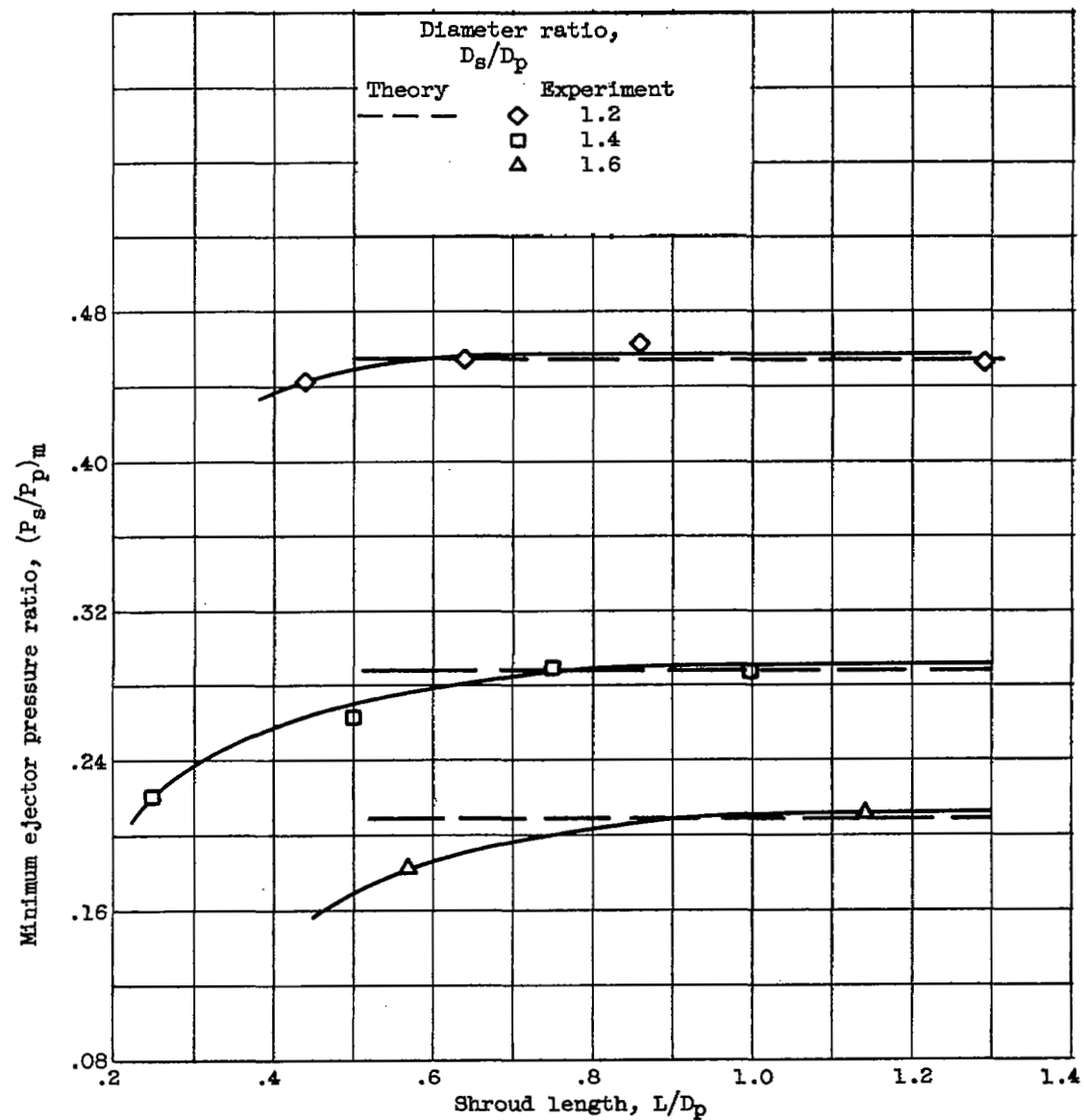
(a) Weight-flow parameter $\omega\sqrt{\tau/\mu}$, 0.045.

Figure 8. - Effect of diameter ratio and shroud length on minimum ejector pressure ratio with secondary flow. Primary specific heat ratio, 1.3; secondary specific heat ratio, 1.4.
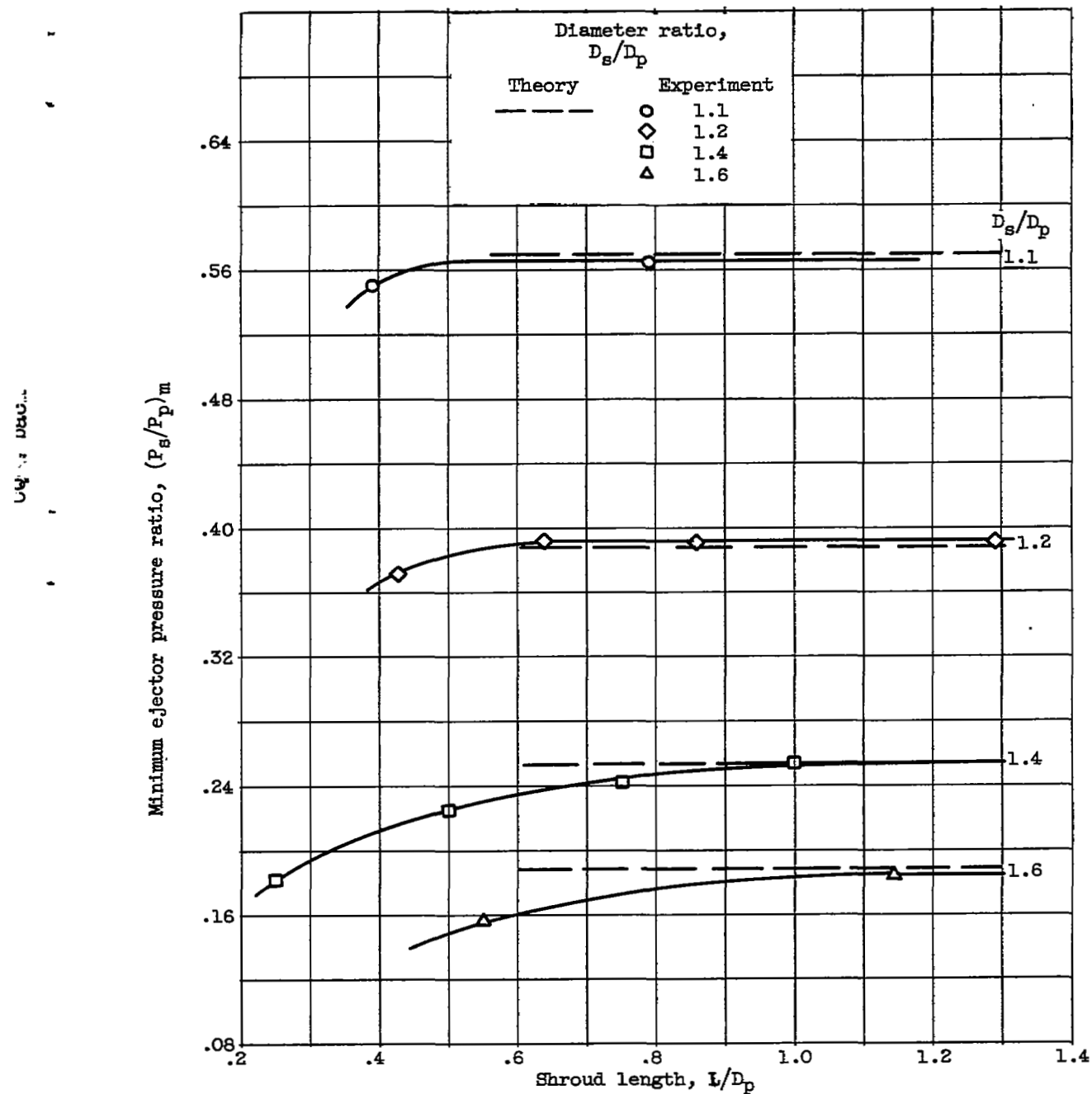
(b) Weight-flow parameter, $\omega\sqrt{\tau/\mu}$, 0.091.

Figure 8. - Continued. Effect of diameter ratio and shroud length on minimum ejector pressure ratio with secondary flow. Primary specific heat ratio, 1.3; secondary specific heat ratio, 1.4.

(c) Weight-flow parameter $\omega\sqrt{\tau/\mu} = 0.135$.

Figure 8. - Concluded. Effect of diameter ratio and shroud length on minimum ejector pressure ratio with secondary flow. Primary specific heat ratio, 1.3; secondary specific heat ratio, 1.4.

3139
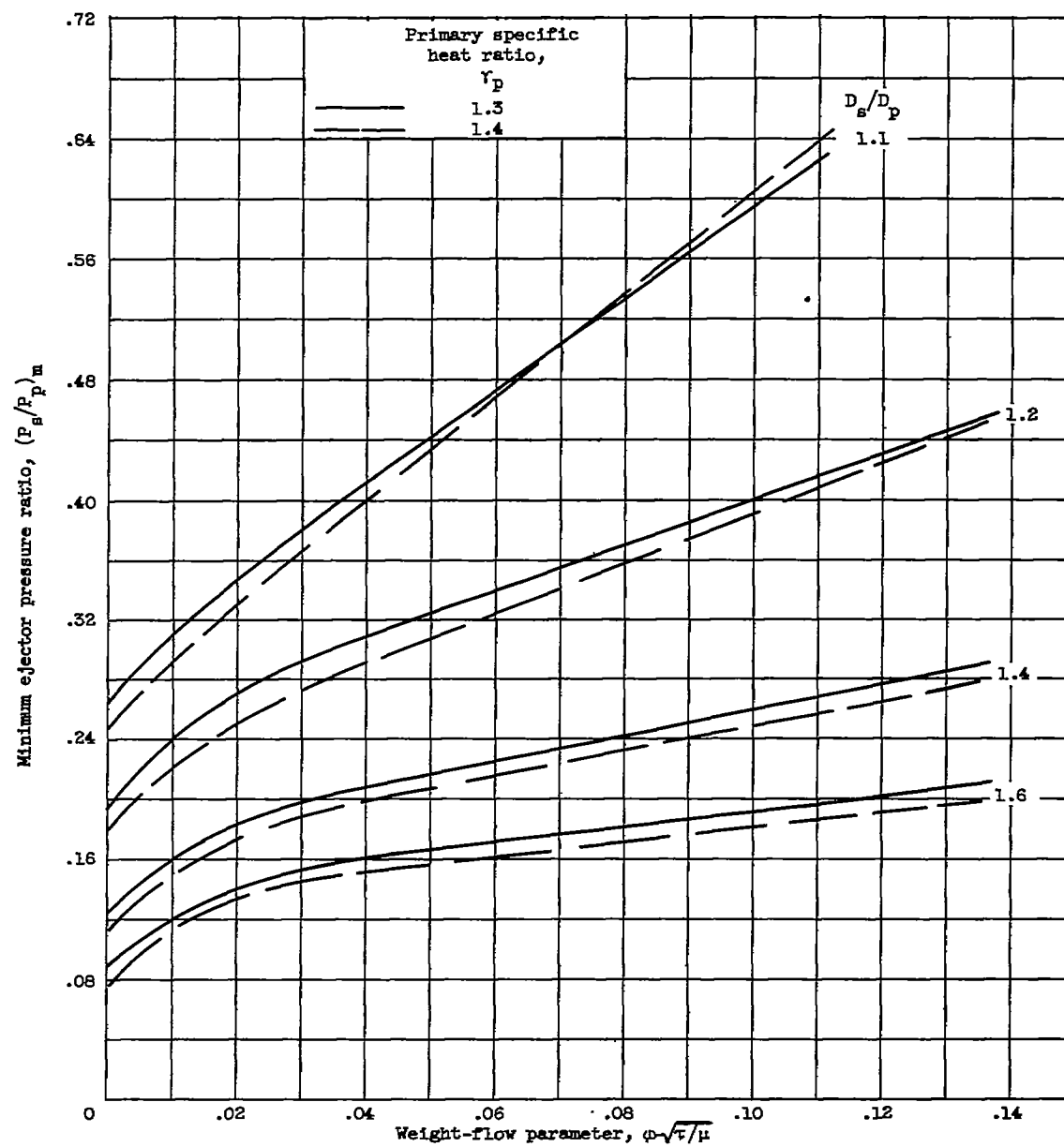
Figure 9. - Theoretical effect of specific heat ratio on minimum ejector pressure ratio.
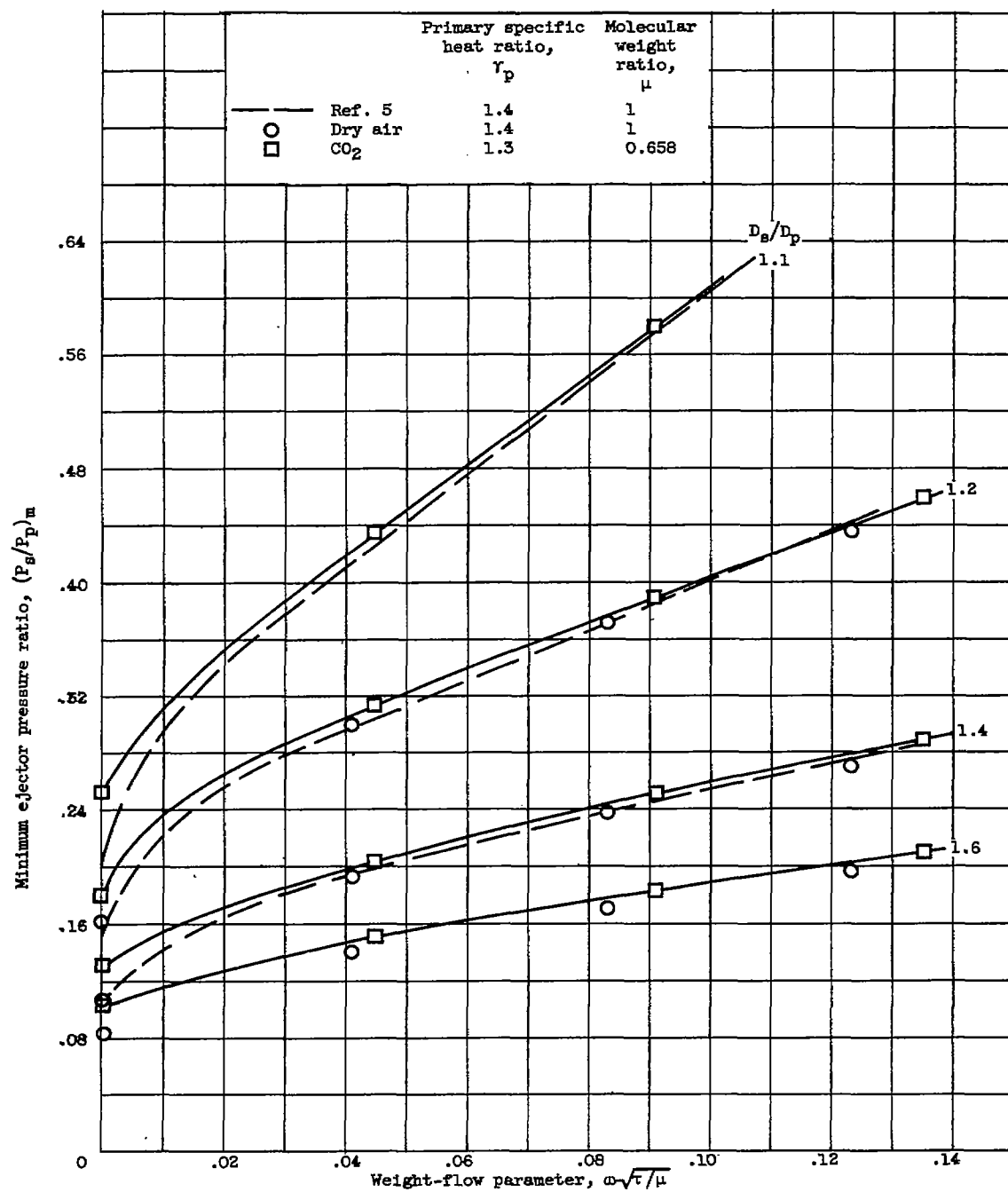
Figure 10. - Comparison of experimental values of minimum ejector pressure ratio for air and carbon dioxide. Temperature ratio, 1; secondary specific heat ratio. 1.4.
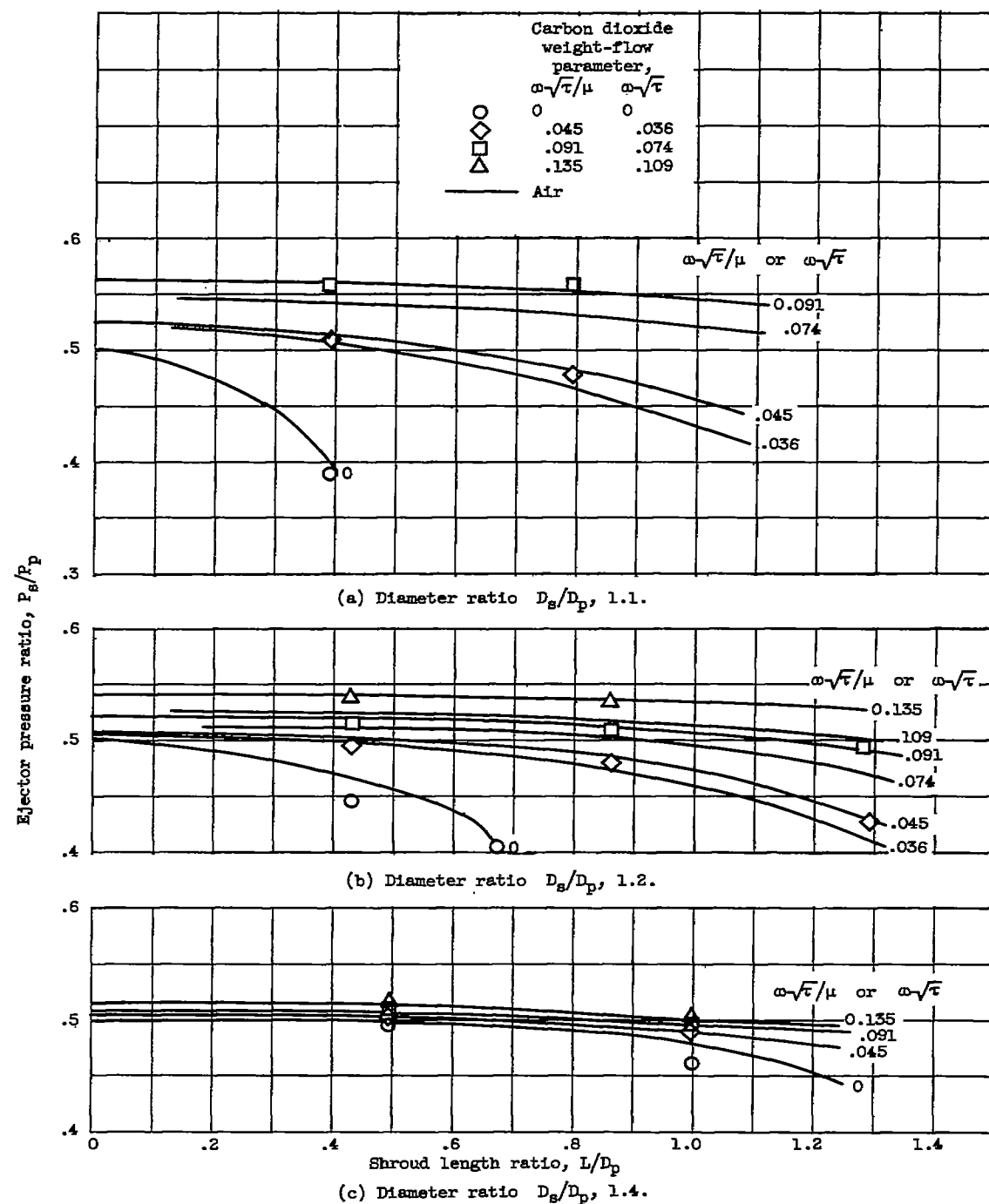
3139

Figure 11. - Effect of primary fluid on ejector performance at high pressure ratio.
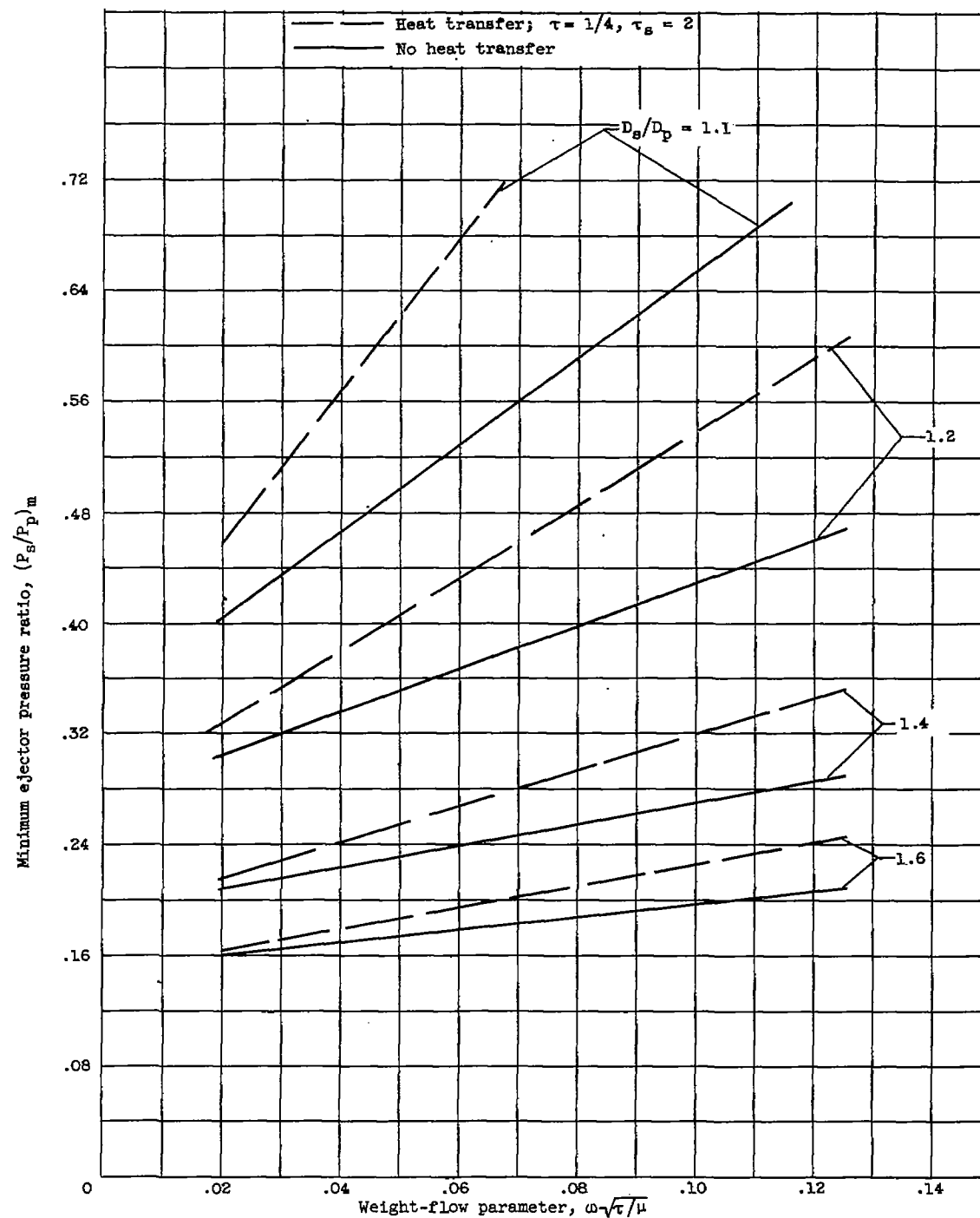Data for air from reference 5.

$P_p/p_o = 2$

Figure 12. - Effect of heat transfer on minimum ejector pressure ratio. Primary and secondary specific heat ratios, 1.4.